

Received October 2, 2018, accepted October 16, 2018, date of publication October 22, 2018, date of current version December 7, 2018.

Digital Object Identifier 10.1109/ACCESS.2018.2877420

Low-Profile Dual-Band Stacked Microstrip Monopolar Patch Antenna for WLAN and Car-to-Car Communications

SHUAI GAO¹, LEI GE¹, (Member, IEEE), DENG GUO ZHANG¹, AND WEI QIN², (Member, IEEE)

¹College of Electronic Science and Technology, Shenzhen University, Shenzhen 518000, China

²School of Electronics and Information, Nantong University, Nantong 226019, China

Corresponding author: Lei Ge (leige@szu.edu.cn)

The work is supported by National Natural Science Foundation of China (No. 61601303), Fundamental Research Foundation of Shenzhen (No. JCYJ20170817095519575).

ABSTRACT In this paper, a low-profile dual-band stacked microstrip monopolar patch antenna is proposed. By utilizing a stacked-patch configuration, a dual-band property is achieved. A coupled annular ring and a set of conductive vias are loaded into the antenna structure to widen the impedance bandwidth. In order to verify the performance of the proposed antenna, a fully functional prototype was fabricated and measured. The measured results demonstrate that the antenna can achieve impedance bandwidths from 2.24 to 2.53 GHz in the low band and from 5.42 to 5.98 GHz in the high band, separately. Within the operating frequency, omnidirectional radiation patterns are also observed. Besides, the proposed antenna possesses a low-profile structure with a height of 4.175 mm or $0.057\lambda_0$ (where λ_0 is the free-space wavelength of 4.1 GHz), which can be easily hidden on the top of a vehicle. With these merits, the proposed design is very appropriate for wireless local area network (2.4–2.48 GHz and 5.75–5.825 GHz) and car-to-car (5.85–5.925 GHz) communications.

INDEX TERMS Low profile, dual-band antenna, monopolar patch antenna, wireless local area network (WLAN), car-to-car (C2C).

I. INTRODUCTION

In wireless communication systems, monopole antennas are widely used to provide a wide signal coverage. However, the height of monopole antennas is $1/4$ wavelength, which is too high for space-limited applications. In 1997, Economou et al. proposed a low-profile circular patch antenna [1]. By directly feeding the antenna at its center, omnidirectional radiation patterns can be obtained. However, the impedance bandwidth of this design is only 1.5%. Therefore, how to widen the bandwidth of this type of antenna is of great concern. In [2], a coupled annular ring is concentrically placed around a center-fed circular patch, and the antenna bandwidth is increased to 12.8%. In [3]–[8], by inserting a set of conductive vias into the antenna configuration to short the radiating patch with the ground plane, the bandwidth of the antenna can be broadened remarkably and a low-profile structure is also achieved.

In the past few years, with the fast development of wireless technologies, wireless local area network (WLAN) and

car-to-car (C2C) communications have been widely used in vehicular communications for internet access and safe driving control. For a moving car on the road, vehicles and base stations are distributed around the car in different directions. In order to communicate with these devices all the time, antennas with omnidirectional radiation patterns are desired to be installed on the car to provide wide signal coverage. In addition, because 2.4/5.8 GHz bands are needed for WLAN and C2C communications are allocated from 5.85 to 5.925 GHz, a single-band antenna [1]–[8] cannot satisfy the above demands. As a result, a dual-band antenna with omnidirectional radiation patterns is required to be installed on the car for WLAN and C2C communications. Recently, different methods are utilized to design this type of antennas [9]–[12]. For instance, by etching eight curved slots on a circular patch [9], a dual-band circularly-polarized microstrip antenna was proposed. However, the bandwidth of this design is only 0.48% in the low band and 0.73% in the high band, which is too narrow to satisfy the requirements of modern wireless

communication systems. Based on dielectric resonator antennas [10], [11], dual-band omnidirectional antennas could also be developed. In [12], an omnidirectional dual-band stacked annular slot/patch antenna was presented. Although these designs could achieve a wider bandwidth [10]–[12], the height of the antennas is not low enough higher than 0.13 free-space wavelength, which limits their applications.

Stacked-patch structure is extensively used in microstrip patch antennas to widen the antenna bandwidth [13]–[15]. However, to the best of the authors’ knowledge, dual-band stacked monopolar patch antennas can hardly be found in open literatures. In [16], a dual-frequency stacked monopolar patch antenna was proposed. By utilizing TM_{01} and TM_{02} modes of a via-loaded ring, a wide impedance bandwidth is generated in the low band. By utilizing TM_{03} mode of the via-loaded ring and TM_{02} mode of a circular patch, the antenna can achieve a wide bandwidth in the high band. Although this work can realize a dual-band property, the high band is tightly related to the low band because the design utilizes TM_{03} mode of the via-loaded ring in the bottom layer to widen the antenna bandwidth in the high band. Therefore, the design can only obtain a fixed frequency ratio of two bands which limits its applications.

In this paper, a low-profile dual-band stacked microstrip monopolar patch antenna is proposed. By utilizing a stacked-patch structure, the antenna is able to operate at two bands and the frequency ratio can be varied according to design requirements. The antenna bandwidth is enhanced dramatically by adding a coupled annular ring and a set of conductive vias into the antenna configuration. To demonstrate the functionality, the proposed antenna was fabricated and measured. Both simulated and measured results reveal that omnidirectional radiation patterns are obtained over two bands. This paper is organized as follows. In Section II, the antenna geometry and operating principle are given, followed with the antenna analysis in Section III. Section IV introduces the results and comparisons with other designs. At last, the conclusion is described in Section V.

II. ANTENNA DESIGN

A. ANTENNA GEOMETRY

The geometry of the proposed antenna is shown in Fig. 1 and the detailed dimensions are given in Table 1. The antenna primarily comprises of Substrate 1, Substrate 2, an upper circular patch, an annular ring, a lower circular patch, a set of conductive vias, a ground plane and a coaxial probe. The upper circular patch whose radius is R_{p0} is printed on the top of Substrate 1 and the lower circular patch with a radius of R_{p1} is printed on the top of Substrate 2. The ground plane has a radius of R_G and it is printed on the bottom of Substrate 2. Substrate 1 is made of Taconic RF-30 with a relative permittivity of 3.0 and Substrate 2 is made of Rogers 5870 with a relative permittivity of 2.33. The thickness of two substrates is H_1 and H_2 , respectively. In order to fix these two substrates together, eight plastic screws are located surrounding the

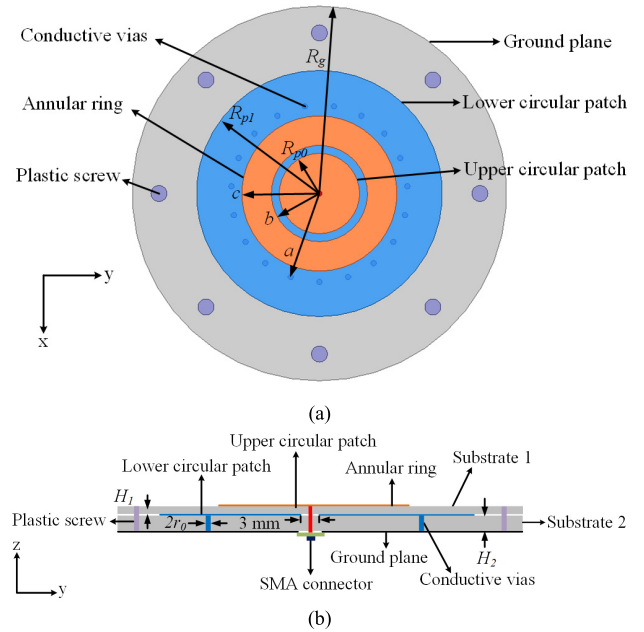


FIGURE 1. Geometry of the proposed antenna. (a) Top view; (b) Side view.

TABLE 1. Dimensions of the proposed antenna.

Parameters	R_G	R_{p0}	R_{p1}	a	b
Values/mm	85	17	46	32.1	17.3
Parameters	c	r_0	H_1	H_2	
Values/mm	30	0.6	1	3.175	

patches. The antenna is simply fed by a coaxial probe with a characteristic impedance of 50 ohm. The inner conductor passes through a clearance hole in the center of the lower circular patch and then directly connects to the upper circular patch center. The diameter of the clearance hole is 3 mm for impedance matching.

In order to widen the antenna bandwidth in the high band, a coupled annular ring is concentrically planed around the upper circular patch. The annular ring has an inner radius of b and an outer radius of c . In order to achieve a wide bandwidth in the low band, a set of conductive vias are inserted into the antenna structure to short the lower circular patch with the ground plane. To be specific, the lower circular patch is shorted by 19 conductive vias which are symmetrically loaded around the z -axis. Each via has a radius of r_0 and each via center is a away from the center of the lower circular patch.

B. OPERATING PRINCIPLE

In this stacked-patch structure, the inner conductor of the coaxial probe directly connects to the center of the upper circular patch, while the lower circular patch is fed by the coupling between the inner probe and the lower circular patch with the clearance hole. This approach leads to a weak

coupling between the resonances of the two circular patches, therefore, a dual-band performance can be achieved.

By adding a coupled annular ring around the upper circular patch, the antenna bandwidth in the high band is broadened dramatically. This is because when the circular patch is excited, the annular ring can be excited at the same time by energy coupling. Due to the size differences between the circular patch and the annular ring, their resonant frequencies are different. By tuning the dimensions of the circular patch, the size of the annular ring and the distance between them, their resonant frequencies can be moved in proximity to each other, then a wide bandwidth can be obtained.

As illustrated in [3], if the substrate thickness is very small compared with the free-space wavelength λ_0 , a circular patch antenna can be considered as a cylindrical cavity. Then a cavity model can be used to analyze the TM_{nm} mode inside the antenna. In terms of [17], the effective radius R_{eff} of the circular patch and the resonant frequency f of the antenna can be calculated as follows.

$$R_{eff} = R \sqrt{1 + \frac{2h}{\pi R \epsilon_r} \left(\ln \frac{\pi R}{2h} + 1.7726 \right)} \quad (1)$$

$$\chi_{nm} = k R_{eff} \quad (2)$$

$$f = \frac{\chi_{nm}}{2\pi R_{eff} \sqrt{\epsilon_r}} \quad (3)$$

Where R is the radius of the circular patch, χ_{nm} is the m th zero of $J'_n(\chi_{nm}) = 0$, k and c are the wavenumber and velocity in the free space, separately.

It is well known that χ_{01} equals to zero, so the resonant frequency of TM_{01} mode is zero according to (3). Consequently, if a monopolar patch antenna is directly fed at its center, the bandwidth is very narrow since the antenna only works in TM_{02} mode. In order to widen the antenna bandwidth, a set of conductive vias can be loaded into the antenna structure to generate a non-zero resonant frequency for TM_{01} mode [3]. Together with original TM_{02} mode generated by the circular patch, the antenna bandwidth can be broadened dramatically.

III. ANTENNA ANALYSIS

A. ANNULAR RING

As illustrated in Section II, the antenna bandwidth in the high band is broadened significantly by adding a coupled annular ring around the upper circular patch. Fig. 2 gives the simulated reflection coefficients with and without the annular ring in the high band. From the figure, it can be observed that the antenna bandwidth is 10.9% from 5.4 to 6.02 GHz in the high band if an annular ring is added. But in other cases, when the annular ring is removed from the antenna structure, the antenna cannot be matched and the reflection coefficients shift upwards above -10 dB.

To further demonstrate the working mechanism of the annular ring, simulated surface current distributions on the upper circular patch and the annular ring at 5.5 and 6 GHz are shown in Fig. 3. Compared with that at 5.5 GHz, the currents on the annular ring are stronger at 6 GHz, demonstrating the

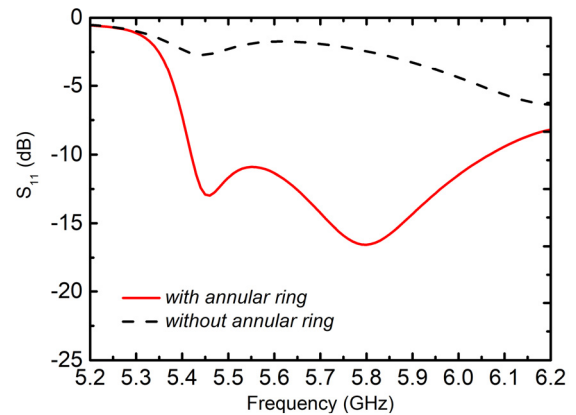


FIGURE 2. Simulated reflection coefficients with and without the annular ring.

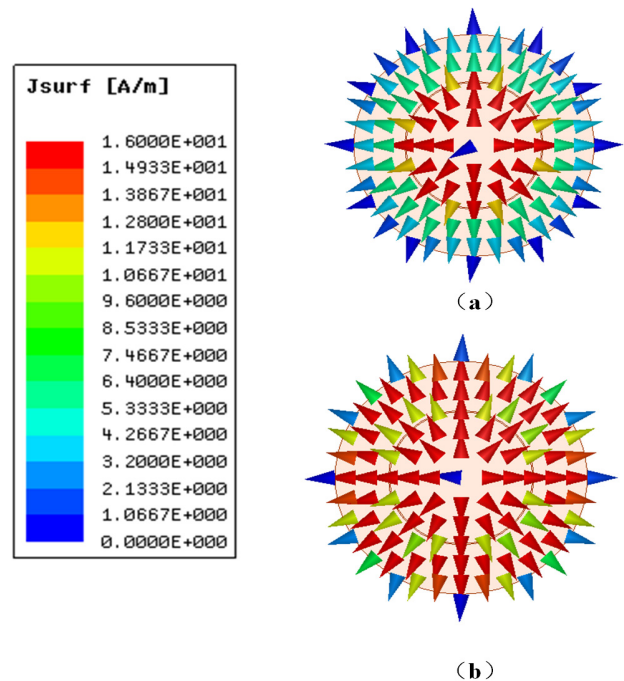


FIGURE 3. Simulated surface current distributions on the upper circular patch and the annular ring: (a) 5.5 GHz; (b) 6 GHz.

annular ring works as a radiator at this frequency. In consequence, a wide bandwidth can be obtained in the high band by adding the annular ring around the circular patch.

B. CONDUCTIVE VIAS

As previously stated, the antenna bandwidth in the low band can be enhanced a lot by adding conductive vias to short the circular patch with the ground plane. Simulated reflection coefficients with and without the conductive vias in the low band are depicted in Fig. 4. It can be seen that when conductive vias are added into the antenna configuration, an impedance bandwidth of 14.2% is realized. However, if the

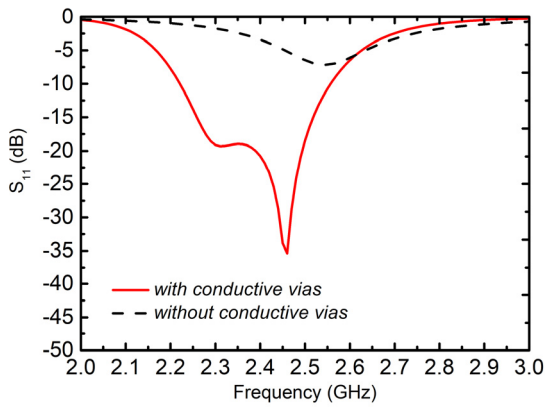
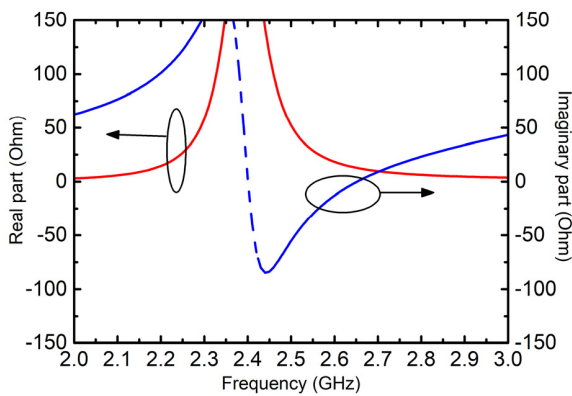
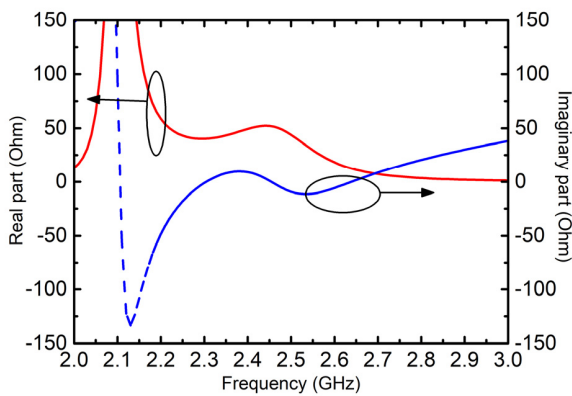


FIGURE 4. Simulated reflection coefficients with and without the conductive vias.



(a)

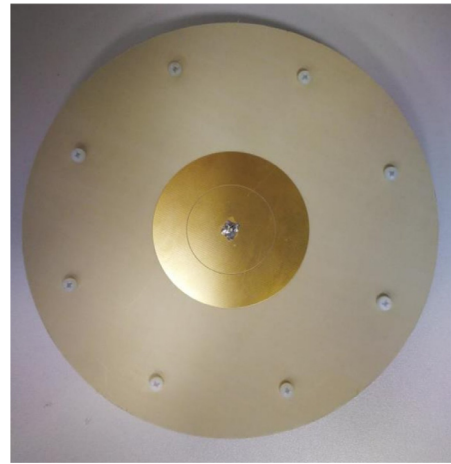


(b)

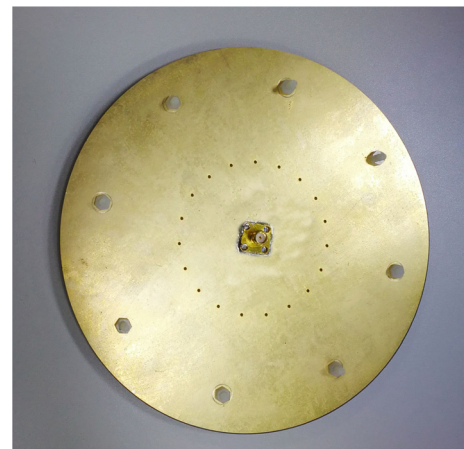
FIGURE 5. Simulated input impedances: (a) without conductive vias; (b) with conductive vias.

conductive vias are removed, the antenna bandwidth becomes deteriorated.

In order to further understand the functionality of the conductive vias, simulated input impedances with and without the conductive vias are given in Fig. 5. From the figure, it can be observed that only a single resonance appears within



(a)



(b)

FIGURE 6. Photograph of the proposed antenna. (a) top view; (b) bottom view.

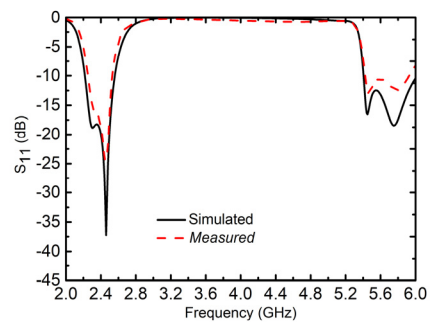


FIGURE 7. Simulated and measured reflection coefficients of the proposed antenna.

the observed frequency band. When the conductive vias are added into the antenna structure, two resonances can be observed within the band. Hence, a wider bandwidth can be achieved when the conductive vias are added.

C. FEEDING METHOD

As depicted in Section II, in this design, the inner conductor of the coaxial probe directly connects to the center of the

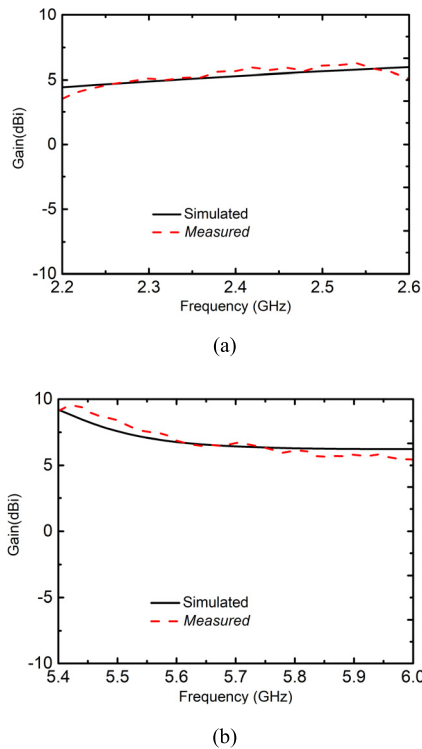


FIGURE 8. Simulated and measured peak gains of the proposed antenna: (a) low band; (b) high band.

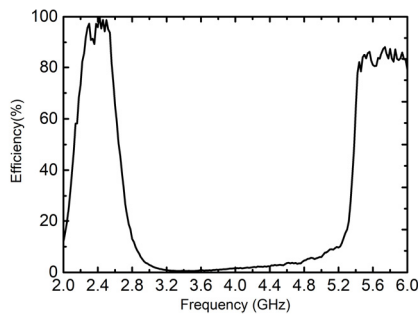


FIGURE 9. Measured total efficiency of the proposed antenna.

upper circular patch, whereas the lower circular patch is fed by the coupling between the inner probe and the lower circular patch with the clearance hole. This feeding method results in a weak coupling between the resonances of the two patches, and then the antenna can operate at two separated bands. In addition, this feeding method allows designers to match the antenna at both bands simultaneously, which facilitates the design procedure.

IV. SIMULATED AND MEASURED RESULTS

A. RESULTS

A fully functional prototype of the antenna was constructed and tested as depicted in Fig. 6 to verify its performance. The simulations were completed by Ansys HFSS. The reflection coefficients (S_{11}), the antenna gains, the radiation

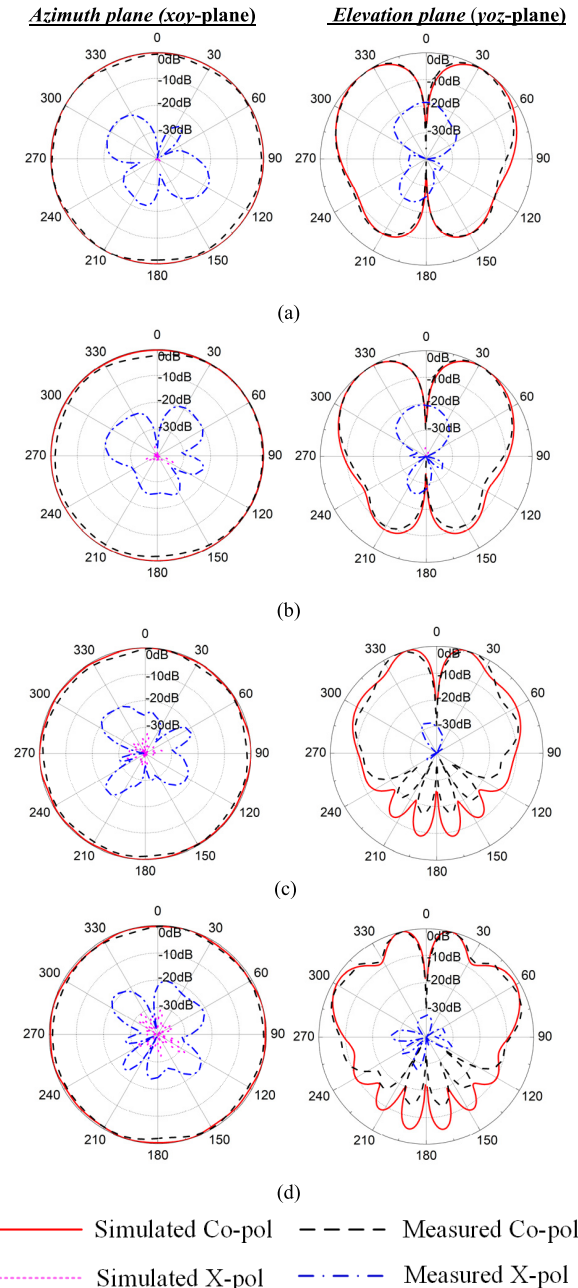


FIGURE 10. Simulation and measurement: radiation patterns: (a) 2.3 GHz; (b) 2.5 GHz; (c) 5.5 GHz; (d) 5.95 GHz.

efficiencies and the radiation patterns were measured by an Agilent E5080A and a near-field measurement system.

The simulated and measured reflection coefficients are shown in Fig. 7. The measurements are in well accordance with the simulations. An impedance bandwidth of 12.2% from 2.24 to 2.53 GHz in the low band and 9.8% from 5.42 to 5.98 GHz in the high band for $S_{11} \leq -10$ dB is measured.

Fig. 8 depicts the simulated and measured peak gains of the proposed antenna. Measured gains agree well with the simulated ones. A measured peak gain of approximately 6 and 7.5 dBi in the low and high band is obtained, respectively.

TABLE 2. Comparison between proposed and reported dual-band omnidirectional antenna.

Ref.	Antenna Type	LF BW/%	HF BW/%	LF	HF	Size
				Peak Gain /dBi	Peak Gain /dBi	
[9]	Patch	0.48	0.73	-	-	$0.34\lambda_0 \times 0.34\lambda_0 \times 0.017\lambda_0$
[10]	Dielectric Resonator	2.64	18.03	-	-	$0.43\lambda_0 \times 0.43\lambda_0 \times 0.18\lambda_0$
[11]	Dielectric Resonator	5.71	7.99	1.3	3.3	$0.89\lambda_0 \times 0.89\lambda_0 \times 0.13\lambda_0$
[12]	Slot/Patch	19.3	18.6	1.3	3.1	$0.6\lambda_0 \times 0.3\lambda_0 \times 0.21\lambda_0$
[16]	Monopolar patch	11.2	13.6	5	6	$1.71\lambda_0 \times 1.71\lambda_0 \times 0.079\lambda_0$
This Work	Monopolar patch	12.2	9.8	6	7.5	$2.32\lambda_0 \times 2.32\lambda_0 \times 0.057\lambda_0$

The total efficiency was also measured by the near-field measurement system, which is shown in Fig. 9. From the figure, it can be observed that the measured total efficiency is more than 80% over the operating frequency. Because the impedance matching is better in the low band and the losses caused by metal and dielectric are low, therefore, the measured total efficiency in the low band is higher than that in the high band. Besides, it should be noted that the antenna measurement system can hardly be very accurate and stable over the high and low frequency bands, which also leads to the difference of the measured efficiency between the two bands.

The simulated and measured radiation patterns of the proposed antenna at 2.3, 2.5, 5.5 and 5.95 GHz are presented in Fig. 10. In the elevation plane, it can be seen that the radiation patterns have a null in 0° and 180° over two bands. Furthermore, the measured cross-polarization levels are below -18 dB in the low band and below -28 dB in the high band. In the azimuth plane, the radiation intensities are nearly the same at every angle and the measured cross-polarization levels are lower than -18 dB at both bands. Hence, the radiation patterns generated by the proposed antenna are similar to ones generated by monopole antennas, which demonstrates the superiority of the design.

B. COMPARISON

The properties of several reported dual-band omnidirectional antennas and the presented design are summarized in Table 2 for comparison. The antenna proposed in [9] has a low-profile structure and the radiation patterns are stable. However, the impedance bandwidths in the low and high band are both less than 1%. The antennas presented in [10]–[12] can obtain a wider bandwidth compared with [9], whereas their heights are more than $0.1\lambda_0$ and the gains are low. The design based on a monopolar patch antenna [16] owns a

low-profile property and a relatively wide bandwidth can also be achieved, but the gain is not high enough and the antenna height is approximately $0.08\lambda_0$. Besides, the high band is tightly related to the low band and only a fixed frequency ratio of two bands can be obtained. In this work, although the design has a larger footprint compared with other types of antennas, a low-profile structure, a fairly wide bandwidth, a relatively high gain and stable omnidirectional radiation patterns can be achieved simultaneously. Besides, it should be mentioned that the ground plane of the proposed antenna can be decreased to further reduce the antenna footprint.

V. CONCLUSION

A novel low-profile dual-band stacked monopolar patch antenna has been presented in this paper. A fully functional prototype was designed, fabricated and measured. Both simulations and measurements prove that omnidirectional radiation patterns can be obtained over two bands. In addition, the antenna also has a low-profile structure. Combined with these advantages, the proposed design is very suitable to be used for WLAN and C2C communications.

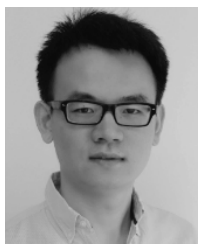
REFERENCES

- [1] L. Economou and R. J. Langley, "Patch antenna equivalent to simple monopole," *Electron. Lett.*, vol. 33, no. 9, pp. 727–728, Apr. 1997.
- [2] A. Al-Zoubi, F. Yang, and A. Kishk, "A broadband center-fed circular patch-ring antenna with a monopole like radiation pattern," *IEEE Trans. Antennas Propag.*, vol. 57, no. 3, pp. 789–792, Mar. 2009.
- [3] J. Liu, Q. Xue, H. Wong, H. W. Lai, and Y. Long, "Design and analysis of a low-profile and broadband microstrip monopolar patch antenna," *IEEE Trans. Antennas Propag.*, vol. 61, no. 1, pp. 11–18, Jan. 2013.
- [4] Y. M. Pan, S. Y. Zheng, and B. J. Hu, "Wideband and low-profile omnidirectional circularly polarized patch antenna," *IEEE Trans. Antennas Propag.*, vol. 62, no. 8, pp. 4347–4351, Aug. 2014.
- [5] Y. Shi and J. Liu, "Wideband and low-profile omnidirectional circularly polarized antenna with slits and shorting-vias," *IEEE Antennas Wireless Propag. Lett.*, vol. 15, pp. 686–689, 2016.
- [6] J. Liu, S. Zheng, Y. Li, and Y. Long, "Broadband monopolar microstrip patch antenna with shorting vias and coupled ring," *IEEE Antennas Wireless Propag. Lett.*, vol. 13, no. 1, pp. 39–42, Jan. 2014.
- [7] T. L. Wu, Y. M. Pan, P. F. Hu, and S. Y. Zheng, "Design of a low profile and compact omnidirectional filtering patch antenna," *IEEE Access*, vol. 5, pp. 1083–1089, 2017.
- [8] H. Wong, K. K. So, and X. Gao, "Bandwidth enhancement of a monopolar patch antenna with v-shaped slot for car-to-car and WLAN communications," *IEEE Trans. Veh. Technol.*, vol. 65, no. 3, pp. 1130–1136, Mar. 2016.
- [9] D. Yu, S.-X. Gong, Y.-T. Wan, and W.-F. Chen, "Omnidirectional dual-band dual circularly polarized microstrip antenna using TM_{01} and TM_{02} modes," *IEEE Antennas Wireless Propag. Lett.*, vol. 13, no. 6, pp. 1104–1107, Jun. 2014.
- [10] Y. M. Pan, S. Y. Zheng, and B. J. Hu, "Design of dual-band omnidirectional cylindrical dielectric resonator antenna," *IEEE Antennas Wireless Propag. Lett.*, vol. 13, pp. 710–713, 2014.
- [11] Y. M. Pan, S. Y. Zheng, and W. Li, "Dual-band and dual-sense omnidirectional circularly polarized antenna," *IEEE Antennas Wireless Propag. Lett.*, vol. 13, pp. 706–709, 2014.
- [12] W. Shi, Z. Qian, and W. Ni, "Dual-band stacked annular slot/patch antenna for omnidirectional radiation," *IEEE Antennas Wireless Propag. Lett.*, vol. 15, no. 2, pp. 390–393, Feb. 2016.
- [13] R. B. Waterhouse, "Design of probe-fed stacked patches," *IEEE Trans. Antennas Propag.*, vol. 47, no. 12, pp. 1780–1784, Dec. 1999.
- [14] H. W. Lai and K. W. Luk, "Wideband stacked patch antenna fed by meandering probe," *Electron. Lett.*, vol. 41, no. 6, pp. 297–298, Mar. 2015.
- [15] X. Yang, L. Ge, J. Wang, and C.-Y.-D. Sim, "A differentially driven dual-polarized high-gain stacked patch antenna," *IEEE Antennas Wireless Propag. Lett.*, vol. 17, no. 7, pp. 1181–1185, Jul. 2018.

- [16] Z. Liang, J. Liu, Y. Li, and Y. Long, "A dual-frequency broadband design of coupled-fed stacked microstrip monopolar patch antenna for WLAN applications," *IEEE Antennas Wireless Propag. Lett.*, vol. 15, no. 4, pp. 1289–1291, Apr. 2016.
- [17] R. Garg, P. Bhartia, I. Bahl, and A. Ittipiboon, *Microstrip Antenna Design Handbook*. Norwood, MA, USA: Artech House, 2001, ch. 5, p. 320.



SHUAI GAO was born in Tieling, Liaoning, China. He received the B.S. degree from Shenzhen University, Shenzhen, China, in 2017, where he is currently pursuing the M.S. degree. His research interests include dual-band antennas and wideband antennas.



LEI GE (S'11–M'15) was born in Xuzhou, Jiangsu, China. He received the B.S. degree in electronic engineering from the Nanjing University of Science and Technology, Nanjing, China, in 2009, and the Ph.D. degree in electronic engineering from the City University of Hong Kong, Hong Kong, in 2015. From 2010 to 2011, he was a Research Assistant with the City University of Hong Kong. From 2015 to 2015, he was a Post-Doctoral Research Fellow with the State Key Laboratory of Millimeter Waves, City University of Hong Kong.

He is currently an Assistant Professor and the Associate Head of the Department of Electronic Engineering, Shenzhen University, China.

His recent research interest focuses on wideband antennas, patch antennas, base station antennas, reconfigurable antennas, millimeter-wave antennas, and filtering antennas. He was a TPC member of the APCAP 2016. He received the Honorable Mention at the Student Contest of 2012 IEEE APS-URSI Conference and Exhibition, Chicago, U.S. He received the 1st Prize in the Student Innovation Competition of 2014 IEEE International Workshop on Electromagnetics, in Sapporo, Japan, in 2014. He was a recipient of the IEEE Antennas and Propagation Society Top 10 Outstanding Reviewer Award from 2017 to 2018.



DENGGUO ZHANG was born in Luzhou, Sichuan, China. He received the B.S. and Ph.D. degrees in electronic engineering from the University of Electronic Science and Technology of China, Chengdu, China, in 1983 and 1988, respectively. After graduation, he has been with the Institute of E.M. and Microwave Technology, Southwestern Communication University, Chengdu, China, as a Lecturer and an Associate Professor since 1991. Then, he joined Shenzhen

University as an Associate Professor and was promoted to be a Full Professor in 1997. He was a Research Fellow with the Department of Electronics Engineering, City University of Hong Kong, from 1993 to 1995 and from 1998 to 1999. From 2002 to 2002, he was a Visiting Scholar with the University of Central Lancashire, U.K. He is currently the Vice Dean of the College of Electronics Science and Technology, Shenzhen University. He has authored two books and over 70 papers, including over 25 papers published in international journals.



WEI QIN (S'09–M'14) was born in Nantong, Jiangsu, China. He received the B.Sc. degree in electronic engineering and the M.Sc. degree in electromagnetic fields and microwave technology from Southeast University, Nanjing, China, in 2007 and 2010, respectively, and the Ph.D. degree in electronic engineering from the City University of Hong Kong, Hong Kong, in 2013.

From 2013 to 2013, he was a Senior Research Associate with the State Key Laboratory of Millimeter Waves, Hong Kong, City University of Hong Kong. Since 2014, he has been with the School of Electronics and Information, Nantong University, Nantong, where he is currently an Associate Professor. His research interest focuses on design and application of microwave devices and antennas.

...